Advances in Aeronautical Science and Engineering
ISSN: 1674-8190

Design and Performance Evaluation of a Ducted Contra-Rotating VTOL UAV

Nkosingiphile Langa| Riaan Stopforth| Daniel Kirkman| Maxim Buzdalov

1. Scientific Multidisciplinary Advanced Research Technologies (SMART) Lab, University of KwaZulu-Natal, KwaZulu-Natal, South Africa, 2. Department of Mechanical Engineering, University of KwaZulu-Natal, KwaZulu-Natal, South Africa, 3. Department of Computer Science, Aberystwyth University, United Kingdom

Abstract:- This study presents the design, fabrication, and experimental evaluation of a cost-effective Contra-Rotating Ducted Unmanned Aerial Vehicle (CRoDUAV) intended for vertical take-off and landing (VTOL) applications in low-resource environments. The prototype integrates mechanical, electrical, and software subsystems into a compact, portable airframe designed for affordability, local manufacturability, and experimental validation. Outdoor flight tests were conducted under angular control using modes such as Stabilize and Altitude Hold (AltHold), where Stabilize provided manual throttle control with angle stabilization, and AltHold added automatic throttle regulation to maintain altitude. Data was collected to assess control performance Results showed successful take-off and hover stability, particularly in yaw and altitude control, with the UAV maintaining a hover between 2 to 3 m above ground. However, limitations emerged in pitch and roll control; in AltHold mode, roll angles often deviated over 35° from commanded values, and pitch exhibited major overshoots and lag. These issues prevented effective control during all five test flights and resulted in multiple crashes. The prototype demonstrated foundational flight capability but lacked robust closed-loop control and stability. This research provides a replicable foundation for CRoDUAV development in emerging technology regions.

Keywords*: CRoDUAV, Vertical Take-Off and Landing (VTOL), Flight Control Systems, Performance Evaluation.*

1. Introduction

Unmanned Aerial Vehicles (UAVs) are flying robots without an onboard pilot. Their versatility and rapidly advancing technological capabilities have made them indispensable across numerous sectors, including aerospace, agriculture, and emergency response [1-4]. The integration of artificial intelligence (AI), the Internet of Things (IoT), and advanced control systems has further expanded their utility in complex missions such as search and rescue, ship inspection, and logistics [5-6]. A notable example is NASA's UAV, Ingenuity, which showcases advanced contra-rotating propulsion systems as it completed over 70 flight missions in the challenging environment of the planet Mars [7-8].

Despite these advancements, the technological development of UAV technology remains gradual, especially in developing countries like South Africa. There has been minimal progress in niche designs such as Contra-Rotating Ducted UAVs (CRoDUAVs) for vertical take-off and landing (VTOL) operations. Factors such as high costs, regulatory barriers, and a shortage of

technical expertise contribute to this lag [9-10]. Efforts from South African universities have demonstrated the potential of UAV development through locally built prototypes, such as the Duo Fugam and Triodactyl [11-12].

Globally, UAV classification lacks standardization, with each country adopting its own regulatory frameworks and categories [12-13]. A basic example of classification is shown in Figure 1 [14]. CRoDUAVs use two rotors and are occasionally grouped under the "tail-sitter" class; however, this classification typically applies to configurations capable of transitioning from vertical to horizontal flight, which requires additional aerodynamic surfaces not present in the developed design [15-18]. The use of a duct while common in some coaxial systems, is not mandatory, but may be included when propeller encasement is desired, serving also as an aerodynamic feature in certain configurations [19-20].

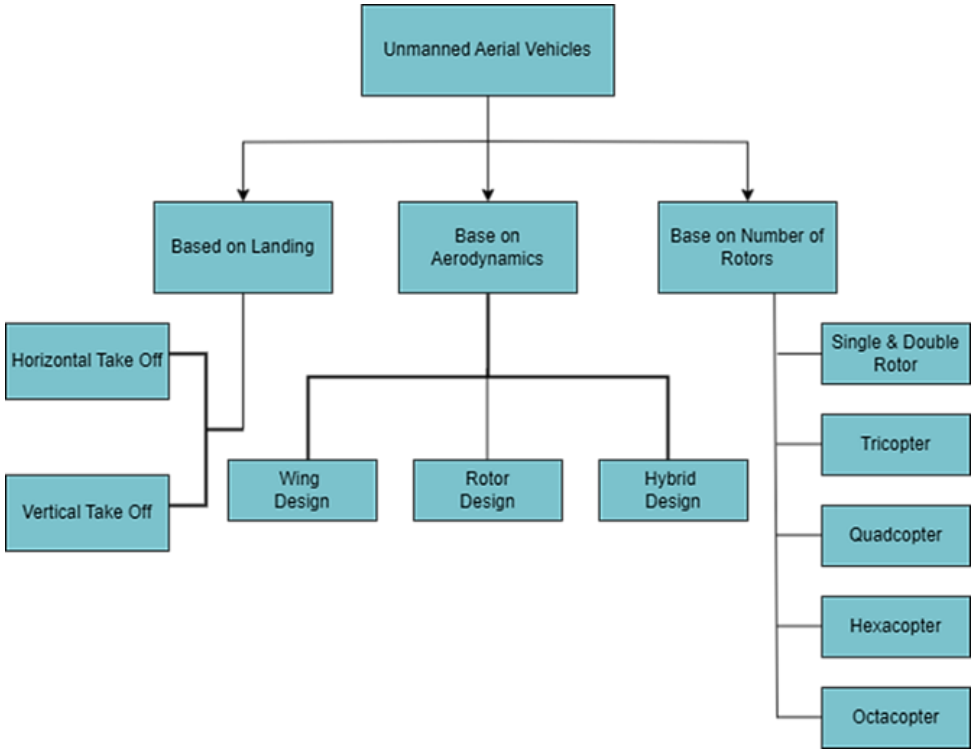

Figure 1: Classification of UAVs base on landing orientation, aerodynamic configuration, and rotor count

CRoDUAV are frequently overlooked due to their complexity in control. Despite their promising advantages a notable knowledge gap continues to exist concerning their aerodynamic efficiency, thrust performance, and control stability across different operational conditions. Current UAV models often face constraints in thrust generation and good manoeuvrability, especially during VTOL operations and low-speed flight. Developments in the 21st century introduced smaller and quieter UAVs; for example, DARPA produced military systems such as the Honeywell T-Hawk MAV, a compact UAV equipped with infrared sensors, and the Aurora Golden Eye 100, capable of carrying a 20-lb payload. Other designs such as iSTAR, GTSpy, and Hovereye were also developed independently, showcasing a variety of UAV designs [21].

2. Objectives and Research Contributions

A cost-effective CRoDUAV prototype was developed, and the aim was to explore its performance in real-world environmental conditions. Prioritizing experimental validation over computational simulations, the study adopts a practical, iterative design process to address core technical challenges. The insights gained contribute to a foundational understanding of CRoDUAV design, with implications for enhanced flight endurance, stability, and operational efficiency.

This study contributes by providing practical, technical, and contextual gaps in CRoDUAV development. Specifically, the key contributions of this work are:

• Development of a cost-effective CRoDUAV prototype tailored for vertical take-off and landing (VTOL) operations, with design decisions tailored for low-resource environments.

• Integration of mechanical, electrical, and software subsystems into a compact, backpack-portable UAV platform, demonstrating manufacturability using accessible tools like 3D printing and laser cut plywood-based structures.

• Real-world experimental validation of the UAV's flight behaviour in both Stabilize and AltHold modes, beyond purely simulation-based approaches common in literature.

• Performance evaluation using detailed flight log data, through analysing of pitch, roll, yaw, and altitude stability using internal control signals (e.g., RCIN, CTUN, BARO, PID errors), which provides transparent insight into the system's limitations.

• Identification of control system deficiencies, particularly in attitude and altitude estimation, highlighting the need for improved PID tuning, actuator configuration, and sensor integration for future development.

• Establishment of a replicable methodology for researchers and engineers in regions with limited access to high-end manufacturing or simulation tools, contributing toward the democratization of UAV development.

3. Materials and Methods

This section outlines the materials, subsystems, and procedures used in the design, construction, and experimental setup of the CRoDUAV prototype.

3.1. System Overview

The prototype design framework combines aspects of mechanical, electrical and software design, to form a cohesive and replicable platform for future research in UAV development (See Figure 2). The system is composed of several interdependent subsystems: the mechanical structure includes the airframe, duct, and control surfaces. The electronics subsystem consists of BLDC motors, electronic speed controllers (ESCs), and servo motors. The software subsystem is anchored by the Pixhawk Flight Management Unit (FMU), which handles control and navigation tasks. Portability was a key consideration in the design, necessitating a compact form factor small enough to fit into a standard backpack. The performance objectives for the prototype included reliable operation in outdoor environments, ensuring flexibility and adaptability in testing conditions.

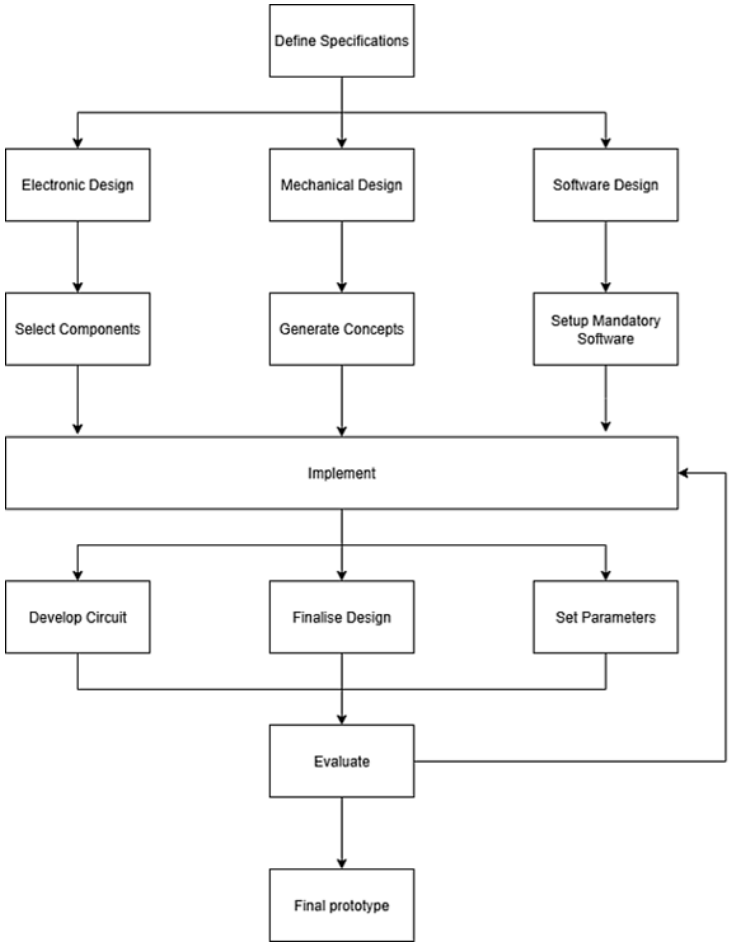

Figure 2: CRoDUAV development methodology illustrating key design stages, subsystem integration, and performance-driven design objectives.

3.2. Design and Modelling

The mechanical design requirements are summarised in Table 1. From various conceptual designs considered, the most feasible prototype was selected, modelled, and developed. SolidWorks was used as the primary Computer-Aided Design (CAD) software for creating the mechanical components. Key mechanical subcomponents designed include the airframe, duct, motor mounting stand, stator, and control surfaces.

The airframe was designed as a stable, lightweight platform to support all mounted components. The O-ring support structures featured an inner diameter of 230 mm to securely house the duct, with an outer diameter of 250 mm. Each ring was equipped with four 30 x 5 mm offset surfaces and cut-ins of 10 x 5 mm (upper) and 20 x 5 mm (lower) to facilitate joint connections to the support legs. These legs, shaped as 140 mm long I-beams, were tailored for structural integrity and attachment accuracy. Two of the legs incorporated 24 x 15 mm slots to house the servo motors. The airframe was constructed entirely from laser-cut 4 mm plywood to simplify manufacturing and ensure material consistency.

The duct, a critical aerodynamic element of the system, was designed to enhance lift and shield the propellers. Its diameter was selected based on preliminary thrust experiments, which identified an optimal propeller size of 203.2 mm (8 inches). To reduce costs and weight, the

duct was fabricated in-house via additive manufacturing (AM) using PLA filament provided by the lab. The CAD model (see Figure 3), with an inner diameter of 225 mm and an outer diameter of 230 mm, was exported in STL format and processed for 3D printing (with an infill density of 40%) using Ultimaker Cura 5.4.0 software.

Table 1: Summary of Key Design Specifications for the CRoDUAV Prototype.

Specification	Explanation
Cost effectiveness	Use of affordable, high strength-to-weight materials and efficient manufacturing methods to minimize development costs.
Ease of use	Simple structural layout to ensure straightforward assembly, operation, and hardware installation.
Manufacturability	Components designed for quick fabrication and easy integration during assembly.
Size	Dimensions based on optimal propeller performance (8-inch propeller configuration); compact enough for portability and overall mass reduction.
Safety	Structural design ensures safe handling and reduces risk of user injury.
Vanes movement	Control surfaces designed to rotate within a 0°–180° range to match servo capabilities.
Weight	Total airframe mass limited to under 1000 g to remain within thrust limits and ensure lightweight configuration post hardware integration.

.

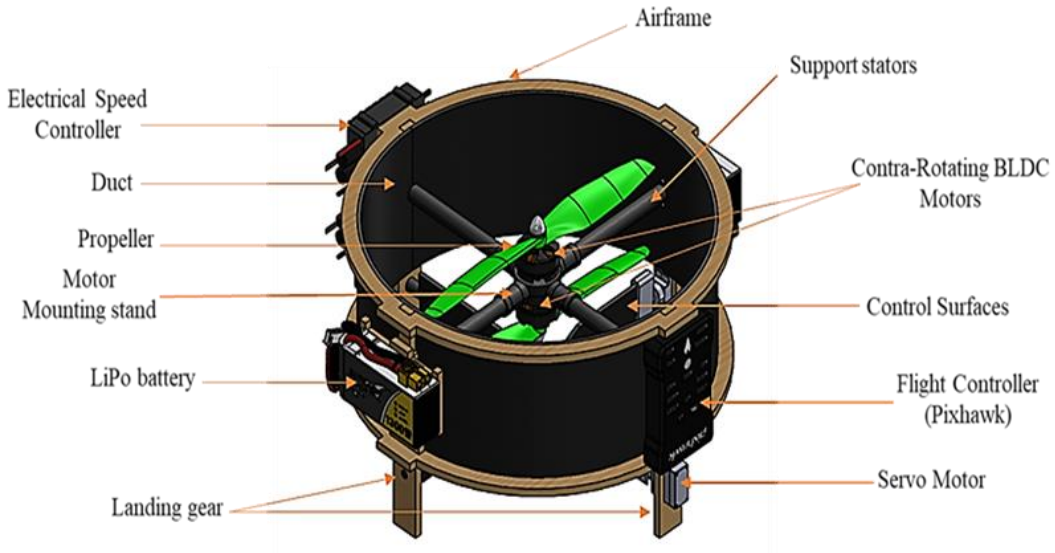

Figure 3: Final CAD model of the CRoDUAV highlighting material selected, structural elements, and electronic hardware placement.

The stator and motor mounting stand functioned as key structural interfaces between the duct, motors, and airframe. Given their placement in high-turbulence zones, rigidity was a primary design objective. Several design iterations were performed to reinforce these parts while minimizing weight. Initially manufactured using AM techniques, the rods were 5 mm in diameter; however, they exhibited bending under stress. A subsequent iteration featured a cross-shaped stator design with 10 mm diameter support rods, significantly improving structural strength and eliminating visible bending.

To further verify structural rigidity, a finite element analysis was performed to evaluate potential high-stress regions. The thrust forces generated by the upper and lower motors were quantified and applied perpendicularly to the motor-mounting stand as 17.64 N each. Figure 4(a) presents the resulting displacement of the motor mount and cross-rods, showing a total deformation of 1.4053 mm under the combined 35.28 N load. While PLA is somewhat weak for this application, the deformation remains small and indicates that the structure can sustain the load without long-term failure.

Elastic strain results in Figure 4(b) show a strain value of 0.006639 m, confirming that the stresses fall within the elastic range and that the structure can recover once the loading is removed. The maximum equivalent stress recorded is 14.767 MPa, well below the typical PLA yield stress of 50–70 MPa, demonstrating that the airframe maintains adequate safety margins under the applied load. Figure 4(c) further displays the equivalent stress distribution, providing mechanical verification that no critical structural weakness or loss of rigidity occurs under the evaluated conditions.

The control surfaces, or vanes, played a pivotal role in manipulating airflow to enhance the UAV's maneuverability. Each vane, 217 mm in length, was designed to be both durable and lightweight to ensure responsive directional control without compromising aerodynamic efficiency. These, along with the servo mounting structures, were produced using the same additive manufacturing process. The flaps, measuring 30 mm wide and 3 mm thick, were precisely matched to the range of motion provided by the servo arms for effective control actuation.

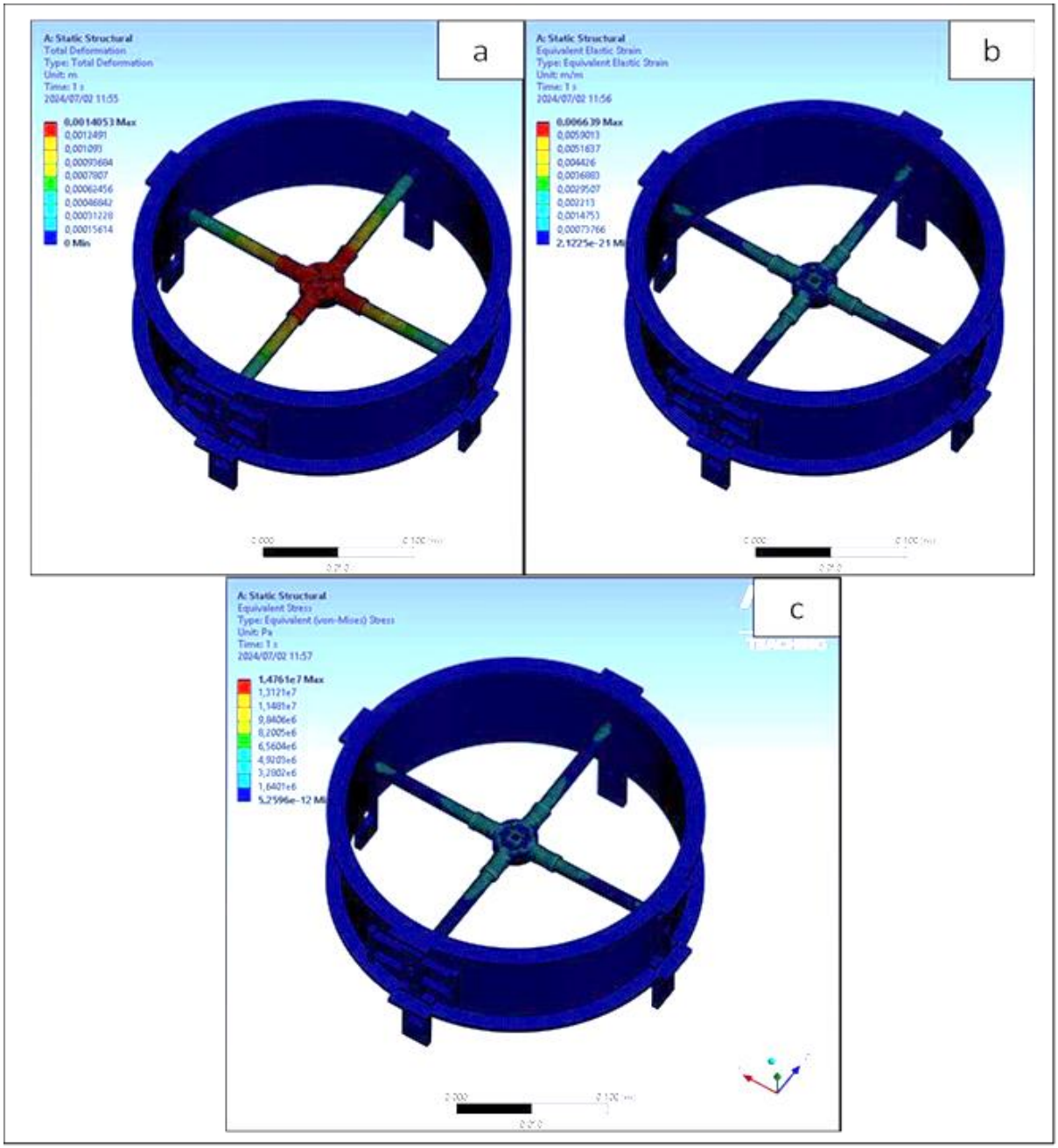

Figure 4:a): Expected total deformation on Cross rods, b) obtained elastic strain results, c) equivalent stress on cross rods.

3.3. Control System and Electronics

The electrical and control architecture of the prototype was carefully designed to support stable flight, real-time responsiveness, and reliable communication between subsystems (see Figure 5). Each component was selected based on a balance of performance, cost-effectiveness, and local availability to ensure the prototype remains replicable for future research or educational use. At the core of the propulsion system is a brushless direct current (BLDC) motor, specifically the T-Motor F60PRO V2.0 Kv1750. This high-efficiency motor was chosen for its excellent thrust-to-weight ratio and reliability, making it ideal for experimental UAV applications. To regulate the motor's operation, a 30 amps Aeolian electronic speed controller

(ESC) was used. This ESC was compatible with the selected BLDC motor and represented a cost-efficient choice among locally available options.

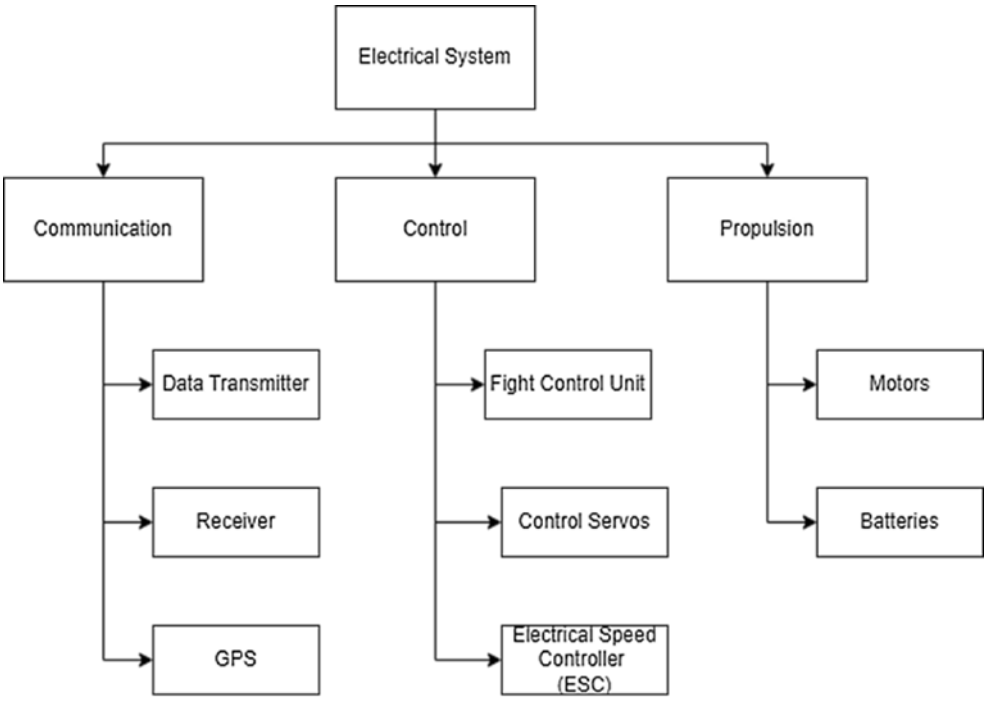

Figure 4: Breakdown of the electrical systems needed to power and control the UAV.

For aerodynamic control, the prototype employed Emax ES08MDII Digital Metal Gear Servos (EMX-SV-0276), which were tasked with actuating the UAV's control surfaces. These servos offer strong torque and digital precision in a compact, lightweight form, making them ideal for real-time flight adjustments. The control system is orchestrated by a Pixhawk 2.4.8 flight management unit (FMU), an open-source and cost-effective autopilot system that integrates sensor data, user input, and control algorithms to stabilize and direct the aircraft. The Pixhawk platform was selected due to its robust support from the open-source community, compatibility with ArduPilot firmware, and low entry cost factors that make it especially suitable for resource-constrained environments.

Communication between the user and the flight controller was facilitated by the FLYSKY FS-i6X 2.4GHz radio transmitter paired with the FS 6CH IA6B receiver. This combination supports the PPM (Pulse Position Modulation) protocol, enabling multiple channels of control through a single input line, which simplifies wiring and reduces latency. Power for the system was supplied by a custom-built 4S battery pack, assembled in-house using Molicel 21700 3.6V 4200mAh Li-Ion cells. This battery solution provided a balance of high energy density and discharge capability, ensuring consistent power delivery during all flight operations.

Before physical integration, the Pixhawk was flashed with *ArduPilot firmware version 4.3.7* using the *Mission Planner* software, a ground control station that allows users to configure UAV parameters via a desktop interface. The flashing process included updating the firmware to multirotor mode and selecting the correct vehicle type to represent the coaxial contra-rotating configuration. Specifically, the parameter *FRAME_CLASS* was set to 9, which corresponds to the *Coax Copter* configuration according to ArduPilot documentation [22]. This value enables

control logic tailored for two vertically stacked, contra-rotating rotors. Following firmware installation, sensor calibration was performed for the onboard accelerometers, gyroscope, compass, and the RC receiver. These calibrations ensured accurate orientation sensing, stable navigation, and correct interpretation of user commands.

To manage stability and safety during flight, three essential flight modes were configured via a three-position switch on the transmitter: *Stabilize, Altitude Hold (AltHold)*, and *Land*. In *Stabilize* mode, the UAV self-levels using gyroscopic data, providing basic attitude stabilization while still allowing full manual control. *AltHold* mode enables the UAV to maintain a consistent altitude automatically, using data from the barometer and accelerometer to adjust motor output. *Land* mode serves as a critical fail-safe, automatically initiating a controlled descent in case of signal loss or pilot command, minimizing the risk of crashes.

During preliminary tests, it was found that fixed control surfaces had minimal impact on turbulent flow, as the lower motor exhibited saturation at maximum PWM signals during throttle increase. To enhance their effectiveness, 4 - fixed square surfaces (40 mm x 40 mm) were installed in the edges of the cross rods, along the centreline housing the motors. The MOT_SPIN_MAX parameter was adjusted to 1 for optimised motor performance and increased inflow to extend hovering time. Additionally, the parameters ATC_ACCEL_P_MAX and ATC_ACCEL_R_MAX, which govern pitch and roll rates, were set to 27000 for better control. Other parameters were increased by 30% to counteract a 29% decrease in PID effectiveness, as detailed in Table 2.

Table 2: ArduPilot Parameters to modify PID values.

Parameter	Pervious value	Modified value
ATC_RAT_PIT_D	0.0036	0.00468
ATC_RAT_PIT_I	0.1	0.13
ATC_RAT_PIT_P	0.5	0.65
ATC_RAT_RLL_D	0.004	0.0052
ATC_RAT_RLL_I	0.1	0.13
ATC_RAT_RLL_P	0.5	0.65
ATC_RAT_YAW_I	0.018	0.0234

Safety protocols were embedded at both software and hardware levels. Pre-flight calibration routines helped ensure all sensors were aligned and operational before take-off, while fail-safes built into the ArduPilot firmware enabled automatic response to loss of signal, battery issues, or out-of-range sensor values. These layers of redundancy were critical in supporting reliable flight performance, especially during initial field trials in dynamic outdoor environments.

3.4. Experimental Setup and Procedure

Testing was conducted iteratively, from preliminary stages to field tests. Due to extensiveness of the iteration process, outdoor tests with a functional final prototype are presented in this study. Each test was organised according to the flight mode being evaluated either Stabilize or AltHold. While the stabilize mode operated on parameters listed in table 2, during AltHold mode PID value were modified to set ATC_RAT {PIT, RLL} _ {P, I} to 0.4, to improve control and reduce/eliminate low-frequency oscillations. Additionally, ATC_INPUT_TC parameter was reduced from 0.15 to 0.1, to improve smoothness of flights, slightly dampen the responsiveness of the prototype to the throttle stick. Since during preliminary tests noise frequencies of around 60 Hz were observed, INS_HNTCH_FREQ parameter was set to 50 (from 80) and INS_HNTCH_BW: set to 10 (from 40), to potentially filter them.

Outdoor Field Tests were carried in the morning on calm, low winds. The procedure for the Stabilize mode tests involved connecting the battery terminals, arming the prototype (fully charged at 16.8 V), gradually increasing the throttle, and applying roll or yaw input as needed to avoid obstacles or maintain balance. Similarly, with the only variation occurring in AltHold mode, where the pilot was required to raise the throttle to achieve lift, then bring it back to the neutral position to maintain altitude autonomously. During each flight, data was collected from onboard Pixhawk sensors and logged via Mission Planner software. Supplementary video footage was recorded using a smartphone for post-test visual verification. Key performance metrics evaluated during testing included altitude stability, pitch and roll behaviour, and overall flight control effectiveness. These metrics were analysed using flight log data and corroborated with observational feedback to assess the prototype's in-flight behaviour and control system performance.

4. Results and discussion

In accordance with the collected results, this section presents findings from flights conducted in Stabilize and AltHold modes. Using log files, performance analysis is also included to evaluate the prototype’s capabilities and highlight its limitations in real-world conditions [23].

4.1. Stabilize mode

Two field tests were conducted under *Stabilize* mode, with the test environment shown in Figure 6. The first test was quickly aborted due to difficulty maintaining control in windy conditions, which significantly compromised the prototype’s maneuverability. As the flight was immediately stopped, data from this run was excluded from the analysis. During the second attempt, the prototype was able to withstand gusts of wind for a short duration before crashing at 56 seconds, which resulted in a fractured leg support on the landing gear. Despite the crash, useful data were captured from the flight logs, specifically the *BARO.Alt* and *CTUN.Alt* parameters (see Figure 7). The *BARO.Alt* value, representing the barometric estimate of altitude based on atmospheric pressure, recorded a peak altitude of 9.21 m. Meanwhile, *CTUN.Alt*, which estimates the flight management unit’s (FMU) internal altitude reading, reported a maximum captured altitude of 9.06 m.

Figure 8 compares the UAV’s Desired Pitch (blue) with the Actual Pitch (orange) during flight in Stabilize mode. While the Desired Pitch remains relatively stable near zero (mean: -0.61°,

min: -3.06°, max: 0.87°), the Actual Pitch shows significant fluctuations, with extreme deviations (mean: -16.73°, min: -73.40°, max: 42.63°). This large discrepancy indicates that the UAV struggled to accurately follow pitch commands, suggesting limited pitch stability and responsiveness. The data shows the prototype's inability to maintain consistent pitch alignment with controller inputs, indicating a critical area for performance improvement.

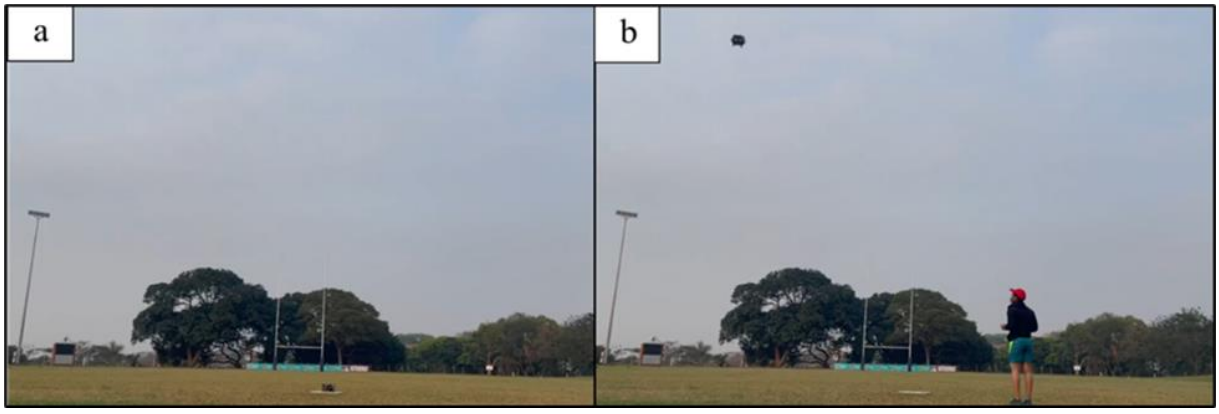

Figure 5: Outdoor Test Environment for CRoDUAV

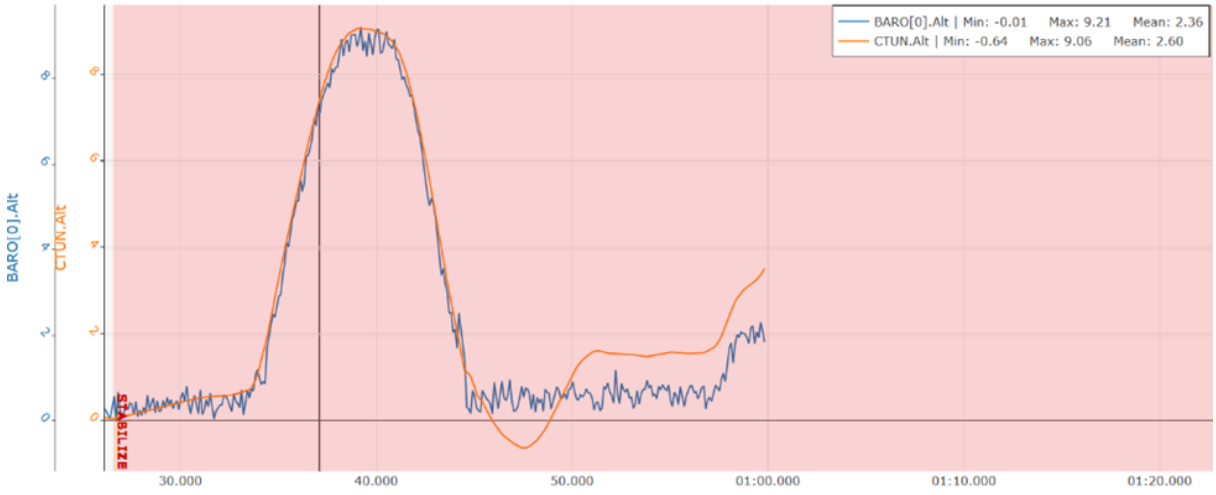

Figure 6: Altitude Comparison Between Barometric Sensor (BARO.Alt) and Flight Controller Estimator.

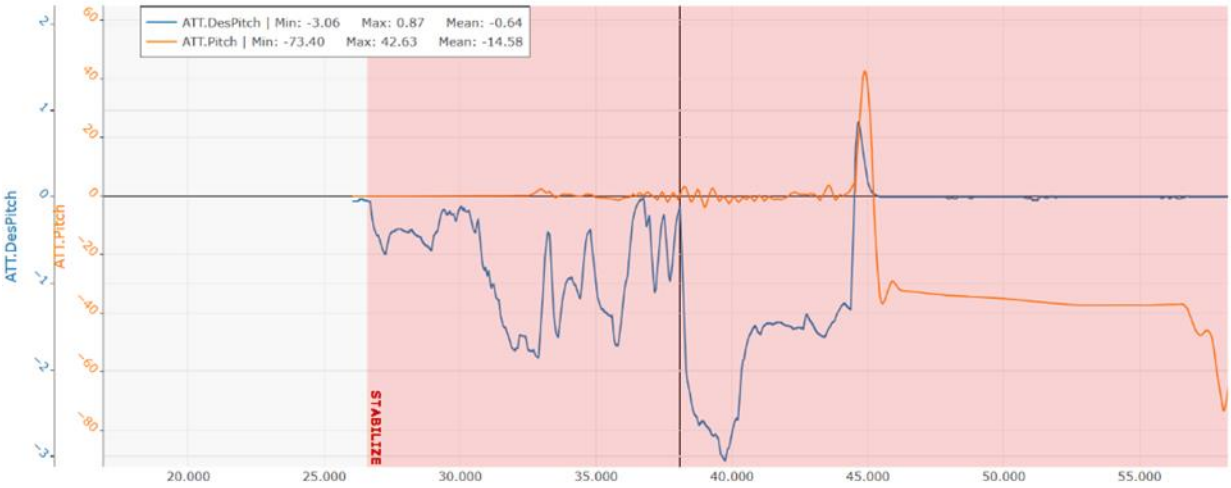

Figure 7: Altitude Control Analysis Showing: Desired vs Actual Pitch.

Figure 9 compares the UAV's Desired Roll (blue line) with the Actual Roll (orange line). While the desired roll remains close to zero throughout the test (mean: -1.13°, range: -7.32° to 0.03°), the actual roll shows significant deviations, with a mean of 31.60° and peaking as high as 124.87°. During the active stabilize flight window (highlighted in red), the UAV was unable to track the controller's roll commands accurately, displaying a major divergence between expected and actual behaviour. The magnitude of the roll deviation also indicates possible mechanical issues or saturation of control surfaces. From the graph it is evident the prototype's inability to maintain roll alignment, pointing to roll control as a major performance limitation.

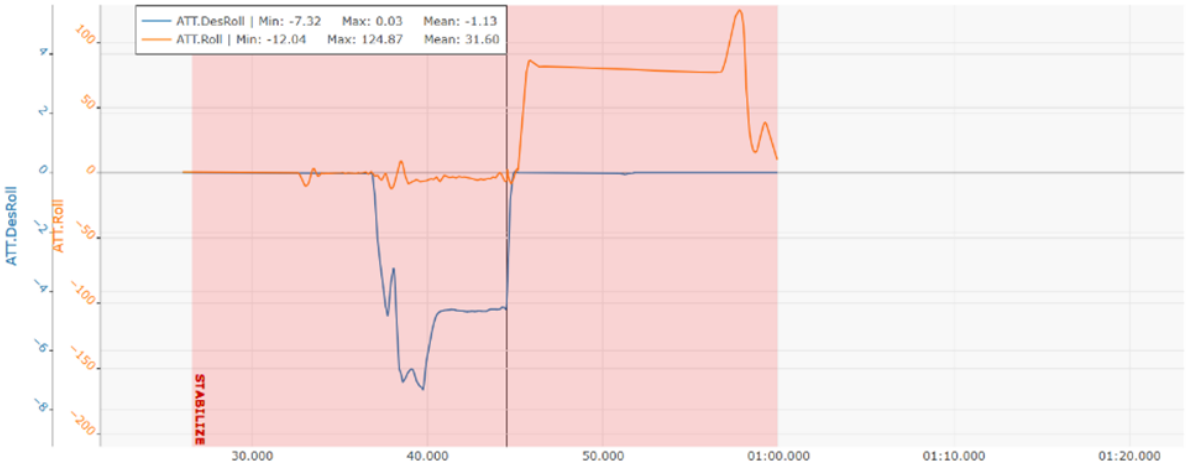

Figure 8: Altitude Control Analysis Showing: Desired vs Actual Roll from Flight Data.

To evaluate the overall flight control effectiveness of the CRoDUAV prototype, the RCIN.C1 and RCIN.C2 (Radio Control Input Channel 1 & 2) input signals were compared against the previously analysed graphs of Desired vs Actual Pitch and Roll. The data show that although the pilot's control inputs (RCIN.C1 for pitch and RCIN.C2 for roll) remained within expected operating ranges, the UAV's actual responses deviated significantly from the desired setpoints. In pitch control, the Actual Pitch demonstrated substantial oscillations and overshoot despite relatively stable input commands, while in roll control, the Actual Roll exhibited extreme deviations even though the Desired Roll remained steady. These mismatches indicate that the

UAV was not effectively translating pilot inputs into controlled movements, suggesting weak tuning of the control system, potential mechanical asymmetries, or insufficient actuation authority. Overall, the flight data reveal that the prototype lacked precise attitude control, leading to poor stability and responsiveness during flight, and demonstrating limited effectiveness of the closed-loop control system.

4.2. AltHold mode

Five additional tests were carried out at the same location to evaluate the CRoDUAV's performance in AltHold mode. Figure 10 compares BARO.Alt (blue) and CTUN.Alt (orange) during flight in AltHold mode. BARO.Alt shows moderate fluctuations around the neutral line (mean: 0.21 m), indicating that the barometric sensor was actively capturing vertical movement. In contrast, CTUN.Alt displays more unsteady behaviour with sharp dips and peaks (min: -9.44 m, max: 2.92 m, mean: -0.70 m). Although the system managed to hold altitude during portions of the flight, the divergence between BARO.Alt and CTUN.Alt highlights areas for improvement in control accuracy and estimation stability. Overall, the UAV showed partial success in maintaining altitude, a stable hover approximately 2–3 m above ground but the data indicates that its vertical control performance was limited and requires refinement.

Figure 11 displays a comparison between the UAV's Desired Pitch (blue line) and Actual Pitch (orange line). While the Desired Pitch remains relatively stable and within a narrow range (min: -21.36°, max: 15.43°, mean: -0.79°), the Actual Pitch shows significant instability, fluctuating sharply across the timeline (min: -89.19°, max: 88.30°, mean: 1.70°). These large deviations indicate that the UAV struggled to follow the controller's pitch commands accurately. Several sharp divergences between the actual and desired values suggest that the control system was unable to maintain consistent pitch alignment. Despite the user's attempts to stabilize the aircraft, the prototype's pitch response was erratic and delayed. Overall, the data indicates that the UAV exhibited poor pitch control performance in AltHold mode, highlighting a critical need for improved tuning and possibly enhanced actuator authority.

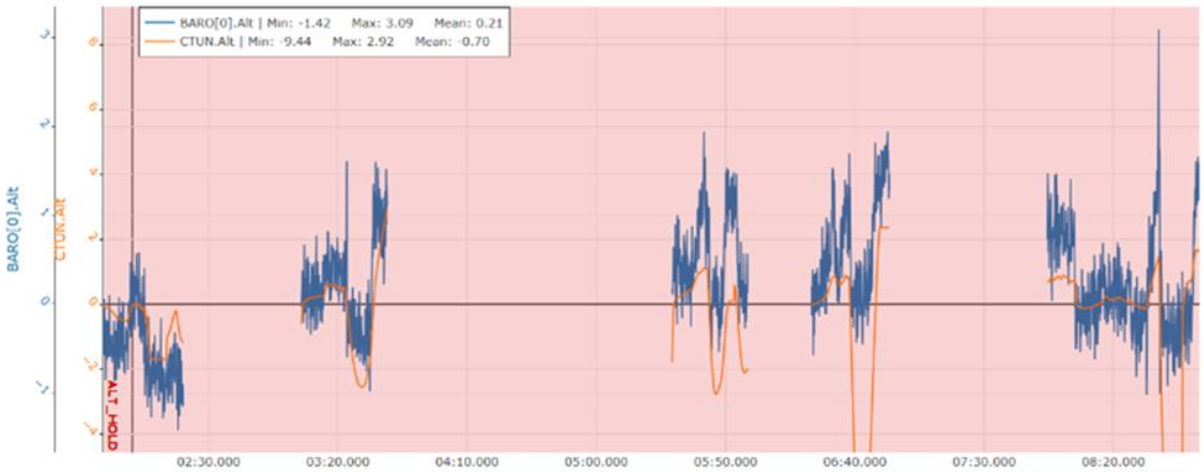

Figure 9: AltHold mode Flight Performance Metrics: Altitude Comparison Between BARO.Alt and CTUN.Alt.

Figure 10: AltHold mode Flight Performance Metrics: Desired vs Actual Pitch.

Figure 12 compares the UAV's Desired Roll (blue line) with the Actual Roll (orange line). The Desired Roll remains mostly stable and close to zero (mean: -0.06°, range: -15.40° to 15.50°), reflecting consistent roll setpoints from the flight controller. In contrast, the Actual Roll fluctuates dramatically, with extreme values ranging from -179.99° to 179.99° and a mean of -35.85°, indicating a severe lack of stability. The frequent and sharp divergences between desired and actual roll suggest that the UAV was unable to maintain roll alignment, even in relatively stable conditions. The data clearly shows that the UAV struggled significantly with roll stability in AltHold mode, confirming that roll control is a critical weakness requiring major refinement in the control system and mechanical configuration.

To deduce the overall flight control effectiveness of the CRoDUAV prototype, RC input signals—particularly RCIN.C1 (pitch) and RCIN.C2 (roll)—were analysed in conjunction with previously presented performance graphs. The data show that although the pilot's control inputs remained within expected operational ranges, the UAV's actual response diverged significantly from the intended commands, indicating limited control accuracy. In altitude control, the comparison between BARO.Alt and CTUN.Alt revealed that while the barometric sensor consistently detected changes in elevation, the controller's internal altitude estimate was unstable, with noticeable drops and spikes suggesting poor tuning or noisy sensor data. In pitch control, although Desired Pitch values stayed within a narrow range, the Actual Pitch fluctuated sharply throughout the flight, reflecting erratic and delayed system response. Similarly, roll control showed a pronounced mismatch, with the Actual Roll experiencing extreme swings far beyond the Desired Roll values, even under steady RC input.

Figure 11: AltHold mode Flight Performance Metrics: Desired vs Actual Roll.

These findings suggest that the flight controller attempted to stabilize the UAV, but the system was unable to execute those commands reliably. The poor correlation between desired and actual UAV motion across all three axes altitude, pitch, and roll indicates that the overall flight control effectiveness of the prototype was limited. This performance gap is likely due to a combination of inadequate PID tuning, mechanical imbalance, actuator limitations, and delayed control feedback, all of which require refinement to achieve stable and responsive flight behaviour.

4.3. Performance Analysis

The recordings and the log files of the tests were all stored and commented on an online repository platform for anyone to access [24]. The following is a tabulated summary of the capabilities and limitation of the CRoDUAV prototype post overall field test log analysis listed on Table 2.

Category	Metric	Result	Interpretation
Pitch Control	Mean actual pitch vs desired pitch	1.70° vs -0.79°	Indicates limited pitch stability and slow response to controller inputs.
Yaw Control	Mean actual yaw vs desired yaw	171.46° vs 179.23°	Stable and responsive yaw control.
Altitude Control	Captured altitude during hover	2–3 m (hover), peak 9 m	Moderate altitude management during take-off and hover.
Orientation Stability	Mean gyroscope X value (GyrX)	-0.07 rad/s	No sustained drift.

Vibration Damping	Mean VibeX	1.43 m/s²	Sensor vibrations within acceptable limits during most flight segments.
Pilot Input Consistency	Mean RCIN.C3 (Throttle channel)	1356.66 µs	Accurate signal transmission and input recognition by the controller.
Power Availability	Mean battery voltage and peak current	14.96 V; 48.7 A	Reliable power delivery for flight operations.
Control Precision (PID)	Mean PID pitch error	0.24	Manually tuned controllers showed inconsistent performance.
Roll Instability	Mean actual roll vs desired roll	-35.85° vs -0.06°	Poor roll control; significant deviation.
High Acceleration Forces	Max AccX	71.96 m/s²	Suggests potential mechanical resonance or unbalanced components.
Excessive Vibration	Max VibeX	70.08 m/s²	Risk of sensor error and instability during vibration spikes.
Motor Saturation	Max RCOU.C5/C6 (motor outputs)	2026 µs	Motors reached maximum command limits; may reflect aggressive control demands or pilot handling issues
Altitude Estimation	Mean CTUN.Alt (altitude estimate)	-0.66 m	Suggests potential barometric sensor miscalibration
PID Inconsistencies	PID error range (roll/altitude)	Large min/max deviations	Occasional instability; indicates need for refined tuning under field conditions.

Table 3: Summary of Performance Metrics Highlighting Capabilities and Limitations of the CRoDUAV Prototype.

5. Conclusions

This study successfully demonstrated the design, fabrication, and experimental validation of a low-cost Contra-Rotating Ducted UAV (CRoDUAV) tailored for VTOL operations in resource-constrained settings. Through iterative prototyping and hardware-in-the-loop field testing, the project achieved several key outcomes aligned with its core research contributions.

The work contributed a replicable and cost-effective CRoDUAV platform, achieved by integrating 3D-printed components, locally sourced electronics, and open-source flight control systems. A practical development methodology focused on manufacturability, material accessibility, and simplified assembly was implemented to ensure feasibility in low-resource environments. The study also established a performance-based approach using real-world

flight logs to assess pitch, roll, and altitude control metrics, providing empirical insights often missing from purely simulation-based research.

Flight trials revealed that the UAV could successfully execute vertical take-off, hover, and yaw stabilization. However, substantial challenges were identified in pitch and roll tracking, primarily due to poor controller tuning and limited actuator authority. Additionally, altitude estimation inconsistencies highlighted the need for more robust calibration and filtering technique.

Overall, this research contributes a valuable baseline for future CRoDUAV studies and offers an adaptable platform for educational or exploratory UAV development. Future work should address identified weaknesses through adaptive PID control, enhanced sensor fusion algorithms, and improved structural rigidity to enable more precise and stable flight behaviour under varying conditions. By demonstrating what is achievable with limited resources, the study supports broader efforts toward democratizing UAV innovation, especially in developing regions.

ACKNOWLEDGMENTS

The authors gratefully acknowledge partial financial support from Council for Scientific and Industrial Research (CSIR), without it this work would not have been possible. They also like to thank the support from the following organisations: Horne Technologies, Stelltron, RS South Africa, and Eskom Tertiary Education Support Programme (TESP). Additionally, the authors acknowledge the use of ChatGPT only as a language editing tool.

Conflict of Interest

The authors declare no conflict of interest.

REFERENCES

[1] Kotarski, D. et al. (2023). Multirotor UAV-A Multidisciplinary Platform for Teaching Mechatronics Engineering. *Sensors*, doi: 10.20944/preprints202306.1725.v1.

[2] L. Marconi and R. Naldi (2012). Control of Aerial Robots: Hybrid Force and Position Feedback for a Ducted Fan. *IEEE Control System*, vol. 32, no. 4, pp. 43–65, doi: 10.1109/MCS.2012.2194841.

[3] Mohsan, S. A. H. et al. (2023). Unmanned aerial vehicles (UAVs): practical aspects, applications, open challenges, security issues, and future trends. *Intelligent Service Robotics*, 16(1), 109–137. https://doi.org/10.1007/s11370-022-00452-4.

[4] Singh, B. (2024). Unmanned Aircraft Systems (UAS), Surveillance, Risk Management to Cybersecurity and Legal Regulation Landscape. *In Unmanned Aircraft Systems*, (pp. 313–354). Wiley. https://doi.org/10.1002/9781394230648.ch8.

[5] Mahobiya, C. et al. (2024). Navigating the Future. *In Unmanned Aircraft Systems*, (pp. 355–385). Wiley. https://doi.org/10.1002/9781394230648.ch9

[6] Wang, J. et al. (2023). Applications, Evolutions, and Challenges of Drones in Maritime Transport. *Journal of Marine Science and Engineering*, 11(11), p.2056. doi: 10.3390/jmse11112056.

[7] Zhao, P. et al. (2023). Review of Key Technologies of Rotary-Wing Mars UAVs for Mars Exploration. *Inventions*, 8(6), p.151. doi: 10.3390/inventions8060151.

[8] Jackson, B., et al. (2025). Profiling Near-surface Winds on Mars Using Attitude Data from Mars 2020 Ingenuity. *The Planetary Science Journal*, 6(1), 21. https://doi.org/10.3847/PSJ/ad8b41

[9] Sibanda, M. et al. (2021). Application of drone technologies in surface water resources monitoring and assessment: A systematic review of progress, challenges, and opportunities in the global south. *Drones*, 5(3), p.84. doi: 10.3390/drones5030084.

[10] Stopforth, R. (2021). VLOS and BVLOS RPAS Operators Certificate: Case Study for Inspection Requirements. *Rapid Product Development Association of South Africa - Robotics and Mechatronics - Pattern Recognition Association of South Africa: Digital Manufacturing: Industrialising Africa, RAPDASA-RobMech-PRASA 2021, Institute of Electrical and Electronics Engineers Inc*., 2021. doi: 10.1109/RAPDASA-RobMech-PRAS53819.2021.9829182.

[11] R. Stopforth, S. et al. (2017). Design considerations of the duo fugam dual rotor UAV. *Pattern Recognition Association of South Africa and Robotics and Mechatronics International Conference, PRASA-RobMech*, vol. 2018-January, pp. 7–13, 2017, doi: 10.1109/RoboMech.2017.8261115.

[12] Harcus, M., and G. Bright,G. (2020). Fused deposition modelling for fabrication of a hybrid vertical take-off and landing unmanned aerial vehicle. *International SAUPEC/RobMech/PRASA Conference, SAUPEC/RobMech/PRASA*, doi: 10.1109/SAUPEC/ROBMECH/PRASA48453.2020.9040964.

[13] Rauhala, A., et al. (2023). An overview of unmanned aircraft systems (UAS) governance and regulatory frameworks in the European Union (EU). *In Unmanned Aerial Systems in Agriculture* (pp. 269–285). Elsevier. https://doi.org/10.1016/B978-0-323-91940-1.00012-8

[14] Anush Lakshman, S., and Ebenezer, D. (2023). Integration of internet of things and drones and its future applications. *Materials Today: Proceedings*, 47, 944–949. https://doi.org/10.1016/j.matpr.2021.05.039.

[15] Dominguez, V. H., et al. (2022). Micro Coaxial Drone: Flight Dynamics, Simulation and Ground Testing. *Aerospace*, 9(5), 245. https://doi.org/10.3390/aerospace9050245.

[16] Filippone, A. (2023). Historical development of the coaxial contra-rotating propeller. *The Aeronautical Journal,* 127(1311), 699–736. https://doi.org/10.1017/aer.2022.92.

[17] Cai, J. et al. (2024). Development of a tube-launched tail-sitter unmanned aerial vehicle. *International Journal of Micro Air Vehicles*, 16. https://doi.org/10.1177/17568293241254045.

[18] Denton, H. et al. (2025). System identification of a thrust-vectoring, coaxial-rotor-based gun-launched micro air vehicle in hovering flight. *International Journal of Micro Air Vehicles*, 17. https://doi.org/10.1177/17568293251361078.

[19] Cheng, Z. et al. (2020). Neural-Networks Control for Hover to High-Speed Level-Flight Transition of Ducted Fan UAV with Provable Stability. *IEEE Access*, 8, 100135–100151. https://doi.org/10.1109/ACCESS.2020.2997877.

[20] Liu, L., & Mi, (2025). Lift–Thrust Integrated Ducted-Grid Fusion Configuration Design for a Ducted Fan Tail-Sitter UAV. *Applied Sciences*, 15(14), 7687. https://doi.org/10.3390/app15147687.

[21] Marconi, L., & Naldi, R. (2012). Control of aerial robots: Hybrid force and position feedback for a ducted fan. *IEEE Control Systems,* 32(4), 43–65. https://doi.org/10.1109/MCS.2012.2194841

[22] Ardupilot.(2025). SingleCopter and CoaxCopter, Https://Ardupilot.Org/Copter/Docs/Singlecopter-and-Coaxcopter.Html.

[23] Ardupilot. (2025). Complete Parameter List. Https://Ardupilot.Org/Copter/Docs/Parameters-Copter-Stable-V4.3.7.Html#complete-Parameter-List.

[24] Langa, N.(2025). Results from field tests for a Ducted Contra- Rotating VTOL UAV. *Zenodo,* https://doi.org/10.5281/zenodo.16875125.